

The Higher K_{-1} States of Hydrogen Peroxide*

We previously reported (1) the spectrum of hydrogen peroxide between 80 and 700 GHz that originates from transitions between the $K_{-1} = 0, 1,$ and 2 levels of $\tau = 1, 2$ and the $K = 0$ and 1 levels of $\tau = 3, 4$. We have also discussed the analysis of this spectrum to microwave accuracy (~ 0.1 MHz) by means of a centrifugal distortion Hamiltonian in which the only effect of the molecular internal rotation is the $\sim 11\text{-cm}^{-1}$ splitting between the $\tau = 1, 2$ and $\tau = 3, 4$ levels. Because the data set was limited to low K_{-1} , it was not possible to calculate Δ_K , and in our analysis Δ_K was fixed to an earlier value derived from infrared studies. Since Δ_K is highly correlated with the A rotational constant and W , the torsional splitting, inaccuracies in Δ_K severely affect the values of the other two constants and make predicted line frequencies at higher values of K_{-1} much less accurate.

Higher- K_{-1} transitions are observable in the 80- to 700-GHz region, but because they are high J , relatively weak, and mixed with a dense background of lines that originate in low-lying excited torsional states, they are difficult to assign. However, we have assigned and analyzed an excellent fir Fourier transform spectrum of hydrogen peroxide provided to us by Dr. Kelley Chance of the Harvard-Smithsonian Astrophysical Observatory. The results of this analysis, combined with our earlier millimeter and submillimeter work, have made it possible to measure extensive new higher- K_{-1} data in the millimeter and submillimeter spectral range. We have now measured 101 new lines that, added to our original data set, give a total of 284 new lines in the 80- to 700-GHz region and include $K_{-1} = 0, 1, 2, 3, 4$ of $\tau = 1, 2$ and $K = 0, 1, 2, 3$ of $\tau = 3, 4$. We have performed an analysis similar to that of our earlier work.

We previously described both the experimental and theoretical techniques used for our analysis of hydrogen peroxide, and interested readers are referred to Ref. (1) for details. Table I shows our new data, and Fig. 1 displays the total data set in the form of a FORTRAT diagram. It can be seen that our new data are $\Delta J = \pm 1$ and that the branches originate in the terahertz region.

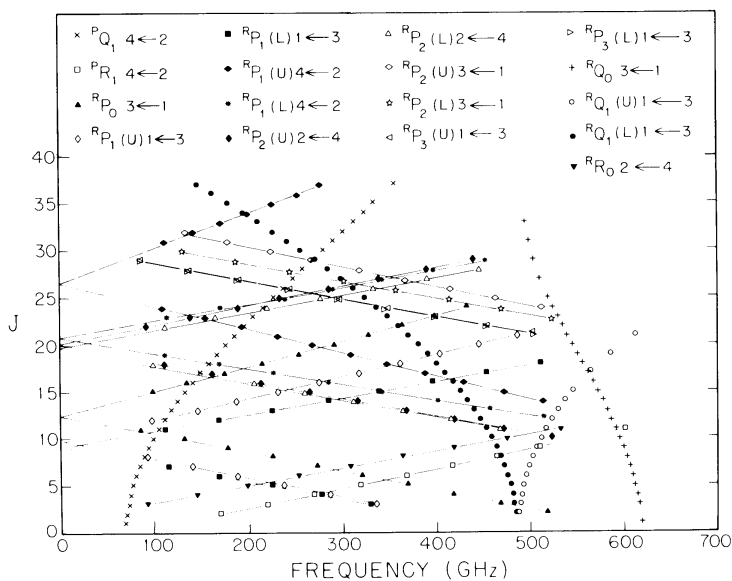


FIG. 1. FORTRAT diagram of the observed branches of HOOH.

* This work supported by NASA Grant NSG-7540.

TABLE I
New Observed Transitions of HOOH (MHz)

R_{F_2} (Upper) Branch Transitions			R_{F_2} (Lower) Branch Transitions		
Transition	Frequency	Observed	Transition	Frequency	Observed
$\tau = 2$	$\tau = 4$		$\tau = 2$	$\tau = 4$	
$9_{97} - 10_{99}$		524 038.11	$10_{97} - 11_{99}$		470 905.39
$10_{98} - 11_{99}$		472 527.24	$11_{98} - 12_{99}$		415 770.2
$11_{98} - 12_{99}$		421 037.05	$12_{98} - 13_{99}$		366 491.74
$12_{99} - 13_{99}$		369 576.78	$13_{99} - 14_{99}$		314 052.03
$13_{99} - 14_{99}$		318 156.12	$14_{99} - 15_{99}$		261 432.50
$14_{99} - 15_{99}$		266 785.43	$15_{99} - 16_{99}$		209 613.97
$15_{99} - 16_{99}$		215 475.52	$16_{99} - 17_{99}$		155 574.84
$16_{99} - 17_{99}$		164 237.48	$17_{99} - 18_{99}$		102 290.96
$17_{99} - 18_{99}$		113 082.96	$18_{99} - 19_{99}$		(48 74.59)
$18_{99} - 19_{99}$		(22 024.01) ^a	$19_{99} - 20_{99}$		(3 006.33)
$19_{99} - 20_{99}$		(11 072.81)	$20_{99} - 21_{99}$		(-9 134.43)
$20_{99} - 21_{99}$		(39 757.85)	$21_{99} - 22_{99}$		113 643.81
$21_{99} - 22_{99}$		90 455.10	$22_{99} - 23_{99}$		168 434.74
$22_{99} - 23_{99}$		141 005.86	$23_{99} - 24_{99}$		223 584.84
$23_{99} - 24_{99}$		191 394.73	$24_{99} - 25_{99}$		279 109.87
$24_{99} - 25_{99}$		241 614.15	$25_{99} - 26_{99}$		335 023.22
$25_{99} - 26_{99}$		291 644.55	$26_{99} - 27_{99}$		391 335.90
$26_{99} - 27_{99}$		341 474.11	$27_{99} - 28_{99}$		448 050.02
$27_{99} - 28_{99}$		391 089.33			
$28_{99} - 29_{99}$		440 476.17			
$29_{99} - 30_{99}$		489 680.66			

R_{F_1} (Upper) Branch Transitions			R_{F_1} (Lower) Branch Transitions		
Transition	Frequency	Observed	Transition	Frequency	Observed
$\tau = 4$	$\tau = 2$		$\tau = 4$	$\tau = 2$	
$12_{111} - 13_{113}$		555 643.40	$11_{99} - 12_{111}$		512 957.60
$13_{112} - 14_{114}$		512 539.44	$12_{99} - 13_{112}$		460 050.87
$14_{113} - 15_{115}$		470 173.32	$13_{99} - 14_{113}$		408 768.92
$15_{114} - 16_{116}$		429 474.90	$14_{99} - 15_{114}$		348 351.11
$16_{115} - 17_{117}$		387 438.99	$15_{99} - 16_{115}$		287 749.51
$17_{116} - 18_{118}$		347 080.11	$16_{99} - 17_{116}$		230 008.34
$18_{117} - 19_{119}$		307 408.38	$17_{99} - 18_{117}$		172 154.47
$19_{118} - 20_{120}$		268 434.20	$18_{99} - 19_{118}$		114 326.92
$20_{119} - 21_{121}$		230 167.83	$19_{99} - 20_{119}$		(-6 486.84)
$21_{120} - 22_{122}$		192 619.92	$20_{99} - 21_{120}$		(1 282.57)
$22_{121} - 23_{123}$		155 801.25	$21_{99} - 22_{121}$		(-8 490.70)
$23_{122} - 24_{124}$		119 722.49	$22_{99} - 23_{122}$		114 389.45
$24_{123} - 25_{125}$		(84 394.50)	$23_{99} - 24_{123}$		173 613.44
$25_{124} - 26_{126}$		(49 828.12)	$24_{99} - 25_{124}$		230 540.37
$26_{125} - 27_{127}$		(15 034.22)	$25_{99} - 26_{125}$		287 111.42
$27_{126} - 28_{128}$		(16 473.47)	$26_{99} - 27_{126}$		343 267.36
$28_{127} - 29_{129}$		(49 193.19)	$27_{99} - 28_{127}$		399 948.70
$29_{128} - 30_{130}$		(80 605.36)	$28_{99} - 29_{128}$		454 046.56
$30_{129} - 31_{131}$		111 202.63			
$31_{130} - 32_{132}$		140 974.77			
$32_{131} - 33_{133}$		169 611.59			
$33_{132} - 34_{134}$		198 003.20			
$34_{133} - 35_{135}$		226 240.10			
$35_{134} - 36_{136}$		251 612.75			
$36_{135} - 37_{137}$		277 112.13			

R_{F_2} (Upper) Branch Transitions			R_{F_3} (Upper) Branch Transitions		
Transition	Frequency	Observed	Transition	Frequency	Observed
$\tau = 3$	$\tau = 1$		$\tau = 1$	$\tau = 3$	
$23_{321} - 24_{323}$		510 225.92	$20_{417} - 21_{319}$		505 478.05
$24_{322} - 25_{324}$		461 863.54	$21_{418} - 22_{320}$		453 390.22
$25_{323} - 26_{325}$		413 861.31	$22_{419} - 23_{321}$		401 269.10
$26_{324} - 27_{326}$		366 148.00	$23_{420} - 24_{322}$		349 119.63
$27_{325} - 28_{327}$		318 772.89	$24_{421} - 25_{323}$		294 932.33
$28_{326} - 29_{328}$		271 755.29	$25_{422} - 26_{324}$		244 717.54
$29_{327} - 30_{329}$		225 115.02	$26_{423} - 27_{325}$		195 473.45
$30_{328} - 31_{330}$		178 872.17	$27_{424} - 28_{326}$		140 201.53
$31_{329} - 32_{331}$		133 047.01	$28_{425} - 29_{327}$		87 603.39

R_{F_2} (Lower) Branch Transitions			R_{F_3} (Lower) Branch Transitions		
Transition	Frequency	Observed	Transition	Frequency	Observed
$\tau = 3$	$\tau = 1$		$\tau = 1$	$\tau = 3$	
$22_{314} - 23_{321}$		523 378.52	$20_{416} - 21_{318}$		505 076.43
$23_{320} - 24_{322}$		478 587.22	$21_{417} - 22_{319}$		452 862.14
$24_{321} - 25_{323}$		413 351.72	$22_{418} - 23_{320}$		400 583.84
$25_{322} - 26_{324}$		357 684.42	$23_{419} - 24_{321}$		348 236.10
$26_{323} - 27_{325}$		301 540.89	$24_{420} - 25_{322}$		295 813.29
$27_{324} - 28_{326}$		244 820.57	$25_{421} - 26_{323}$		243 308.95
$28_{325} - 29_{327}$		187 616.91	$26_{422} - 27_{324}$		190 715.62
$29_{326} - 30_{328}$		130 227.97	$27_{423} - 28_{325}$		138 026.29

^a Numbers in parenthesis are calculated from the constants of Table II.

TABLE II
Rotational Constants (MHz)

	$\tau = 1, 2$		$\tau = 3, 4$	
	value	σ	value	σ
A	301 874.205	0.037	301 586.074	0.075
B	26 212.439	0.046	26 155.639	0.036
C	25 098.604	0.046	25 186.461	0.036
$\Delta_J (\cdot 10^0)$	0.105292	0.000029	0.0996169	0.000014
$\Delta_{JK} (\cdot 10^{-1})$	0.112180	0.000026	0.115275	0.000051
$\Delta_K (\cdot 10^{-2})$	0.120340	0.00012	0.118558	0.00023
$\delta_J (\cdot 10^3)$	-0.258456	0.0014	0.686780	0.0012
$\delta_K (\cdot 10^{-1})$	0.978631	0.0027	0.638326	0.00021
$H_{JK} (\cdot 10^3)$	0.506307	0.0097	0.0594176	0.0013
$H_{KJ} (\cdot 10^2)$	-0.161735	0.0087	-0.0506399	0.0073
$H_K (\cdot 10^2)$	0.185268	0.097	-----	
$h_J (\cdot 10^7)$	0.304918	0.022	-0.515225	0.011
$h_{JK} (\cdot 10^3)$	0.172789	0.00090	0.129727	0.0011
$h_K (\cdot 10^1)$	0.440464	0.038	-0.631712	0.0028
$L_{JK} (\cdot 10^7)$	-0.159961	0.0045	-0.105713	0.0071
$L_{JK} (\cdot 10^5)$	-0.933110	0.051	0.829787	0.0077
$L_{KKJ} (\cdot 10^4)$	0.218515	0.038	-----	
rms		0.126		0.112
number of data points		119		141
W				342 881.62

The analysis of hydrogen peroxide is complex because of the effects of the torsional motion. This motion splits the ground vibrational state into two pairs of sublevels, $\tau = 1, 2$ and $\tau = 3, 4$, and gives the selection rules, $\tau = 1 \leftrightarrow 3$ and $\tau = 2 \leftrightarrow 4$, in addition to the usual asymmetric rotor restrictions. As before, we analyze the lower $\tau = 1, 2$ levels by means of combination differences connected in the $\tau = 3, 4$ state. We assume that the rotational constants in $\tau = 1$ and $\tau = 2$ are the same and find that the 119 distinct combination differences can be analyzed with an rms deviation of 0.13 MHz. The values of the constants that result from this analysis are shown in Table II. Fewer combination differences exist in $\tau = 3, 4$, so we supplement these data. Additional energy levels in $\tau = 3, 4$ are calculated from combination of the energy levels produced by the $\tau = 1, 2$ analysis with measured transition frequencies between $\tau = 1, 2$ and $\tau = 3, 4$. We are careful to use only $\tau = 1, 2$ states that we believe to be well established. The effect of this procedure is that some lines at high J (>30) are not used in the analysis because they were not part of the $\tau = 1, 2$ analysis and that these transitions may not be reproduced to microwave accuracy. While it would be possible to include them in the analysis, we feel that this is undesirable because the $\tau = 3, 4$ analysis would have to readjust its constants to cancel extrapolation errors in the $\tau = 1, 2$ analysis. The results of the $\tau = 3, 4$ analysis are also shown in Table II.

With our new measurements the characterization of the rotational-torsional spectrum of the $\tau = 1, 2, 3, 4$ states of hydrogen peroxide in the spectral region below 700 GHz is virtually complete. Most transitions between thermally populated energy levels have been directly measured and those that have not (these are mostly low-frequency lines below 100 GHz) can be calculated from our centrifugal distortion analysis with high accuracy. This work also impacts work in both the fir and ir spectral

regions. In the fir the results of our analysis of microwave data predict the higher- K_{-1} data of the fir to the accuracy of those data. These analyses also provide strong ground state constraints and starting points for several very interesting (2, 3) analyses of ir data now in progress.

REFERENCES

1. P. HELMINGER, W. C. BOWMAN, AND F. C. DE LUCIA, *J. Mol. Spectrosc.* **85**, 120–130 (1981).
2. J. HILLMAN, private communication.
3. W. B. OLSON, Thirty-Fifth Symposium on Molecular Spectroscopy, Ohio State University, Columbus, 1980, paper TE6.

WAYNE C. BOWMAN
FRANK C. DE LUCIA

*Department of Physics
Duke University
Durham, North Carolina 27706*

PAUL HELMINGER

*Department of Physics
University of South Alabama
Mobile, Alabama 36688
Received December 8, 1980*